A data-based mathematical modelling study to quantify the effects of ciprofloxacin and ampicillin on the within-host dynamics of *Salmonella enterica* during treatment and relapse

1. Myrto Vlazaki[1] (*)

2. Omar Rossi[2]

3. David J. Price[3,4]

4. Callum McLean[1]

5. Andrew J. Grant[1]

6. Pietro Mastroeni[1]

7. Olivier Restif[1]

[1]Department of Veterinary Medicine, University of Cambridge, Madingley Road, CB3 0ES

[2]GSK Vaccines institute for Global Health, Via Fiorentina 1, 53100, Siena (Italy)

[3]Centre of Epidemiology and Biostatistics, University of Melbourne, Grattan Street, Parkville, Victoria, 3010, Australia

[4]The Doherty Institute for Infection and Immunity, 792 Elizabeth Street, Melbourne, Victoria, 3000, Australia

(*) Corresponding Author e-mail address: mv382@cam.ac.uk

Keywords: mechanistic model, data-based model, model selection, isogenic tagged strains, bacterial persistence, heterogeneity

Abstract

Antibiotic therapy has drastically reduced the mortality and sequelae of bacterial infections. From naturally-occurring to chemically-synthesised, different classes of antibiotics have been successfully used without detailed knowledge of how they affect bacterial dynamics *in vivo*. However, a proportion of patients receiving antimicrobial therapy develop recrudescent infections post-treatment. Relapsing infections are attributable to incomplete clearance of bacterial populations following antibiotic administration; the metabolic profile of this antibiotic-recalcitrant bacterial subpopulation, the spatiotemporal context of its emergence and the variance of antibiotic-bacterial interactions *in vivo* remain unclear. Here, we develop and apply a mechanistic mathematical model to data from a study comparing the effects of ciprofloxacin and ampicillin on the within-host dynamics of *Salmonella enterica* serovar Typhimurium in murine infections. Using the inferential capacity of our model, we show that the antibiotic-recalcitrant bacteria following ampicillin, but not ciprofloxacin, treatment belong to a non-replicating phenotype. Aligning with previous studies, we independently estimate that the lymphoid tissues and spleen are important reservoirs of non-replicating bacteria. Finally, we predict that post-treatment the progenitors of the non-growing and growing bacterial populations replicate and die at different rates. Ultimately, the liver, spleen and mesenteric lymph nodes are all repopulated by progenitors of the previously non-growing phenotype in ampicillin-treated mice.

1. Introduction

In the modern era, antibiotics are the cornerstone of therapeutics in bacterial disease treatment [1]. The term "antibiotics" refers to a heterogeneous collection of naturally-derived or chemically synthesised compounds which clear bacterial infections through various biochemical mechanisms, including inhibition of cell wall synthesis, bacterial lysis, nucleic acid and protein synthesis inhibition (reviewed in [2]). Antibiotics are traditionally classified as either bactericidal reducing bacterial load by killing bacteria, bacteriostatic acting to limit bacterial loads by keeping bacteria in a stationary growth phase, or both [3-4].

The effect of different antibiotics on bacterial dynamics has been studied extensively *in vitro*, in optimally and homogeneously growing bacterial populations harvested from exponentially growing cultures [5]. Conclusions drawn from these studies provide insights into the mode of action of different antibiotic agents on their bacterial targets; however, their clinical relevance remains unknown, as *in vivo* bacterial populations are characterised by heterogeneity in their growth and dissemination dynamics [6-9]. Upon successful colonisation, *in vivo* bacterial behaviour is multifactorially shaped by nutrient availability [6,10], host immunity [11-13], spatial arrangement of the infectious foci [14], and host cell composition in the immediate bacterial vicinity [15-16]. The landscape of within-host bacterial dynamics is further complicated by the induction of stress responses in bacterial populations exposed to antibiotics, which alter the bacterial metabolic and transcriptional profile, slow down or stop replication, and ultimately affect the pathogen's susceptibility to the antibiotic [17]. These adaptations may lead to incomplete clearance of the bacterial load as a result of the emergence of an antibiotic-recalcitrant, yet genetically non-resistant, bacterial subpopulation, termed "persister" [18-19].

An important caveat of *in vitro* studies using optimally growing bacteria from exponential phase cultures is disregarding the influence of the bacterial growth rate on the therapeutic effect of some classes of antibiotics. All clinically-used antibiotic classes exert their maximum therapeutic effect when applied to optimally growing bacteria, where cidal agents clear 99.9% of the bacterial load under clinically relevant regimens [20-22]. However, *in vitro* studies with *Escherichia coli* and *Staphylococcus aureus* have revealed that even though different antibiotic classes are homogeneously effective on exponential phase bacteria, they exert heterogeneous effects on slowly-replicating and non-replicating bacterial populations. Depending on which

bacterial functions they target, different antibiotic classes are more or less active against slow- or non-replicating bacteria [5, 23-25].

For example, beta-lactam antibiotics (natural and synthetic penicillin-like compounds), like ampicillin, have a range of pharmacological targets including bacterial cell wall synthesis and bacterial autolysis pathways amongst others [26], resulting in both bacteriostatic and bactericidal properties respectively. However, bacteriostatic effects attributable to bacterial cell wall disruption may act antagonistically to the bactericidal effects due to bacterial lysis [26]. This antagonistic relationship has been experimentally observed *in vitro* as a positive correlation between the cidal effect of beta-lactams and the growth status of the targeted bacteria [27-28]. This class of antibiotics induces structural changes in the bacterial peptidoglycan cell wall leading to cell lysis via a bulge-mediated process [29]; whether these morphological changes modulate bacterial replication rates and to what extent this phenotypically static effect antagonises the cidal action of the drug requires further investigation [30].

In contrast, quinolones, like ciprofloxacin, predominantly target the transcriptional machinery of the bacteria, and thus do not slow down bacterial growth at clinically relevant concentrations [31]. They act as DNA gyrase inhibitors, stalling bacterial chromosome replication through the formation of double-strand DNA breaks, thus preventing the replication forks from accessing the terminus [32]. Unlike beta-lactams whose efficacy has been linearly correlated with bacterial growth rate [27-28], quinolones act on heterogeneously growing bacteria so long as they remain transcriptionally active [33]. Unlike other antibiotics the bactericidal activity of ciprofloxacin is not affected by the bacterial growth rate, both in *in vitro* optimally-growing bacterial populations and in *in vivo* bacterial populations displaying heterogeneity in replication rates [23].

Unlike bacteria in cultures, the heterogeneity of bacterial growth dynamics *in vivo* is far greater. A substantial body of literature has been dedicated to studying the *in vivo* effects of antimicrobial therapy on murine infections with *Salmonella enterica* serovar Typhimurium, especially focusing on slow- or non-replicating bacterial cells during antibiotic exposure. Despite the fundamental *in vitro* differences in the modes of action of different antibiotic classes, a large proportion of *in vivo* experimental studies involving naturally-occurring heterogeneously-replicating bacterial populations have been conducted using second-

generation fluoroquinolone agents (either enrofloxacin or ciprofloxacin) in murine infections with *S.* Typhimurium [6, 34-35]. Using fluorescent-based techniques for observation of bacterial dynamics at the single-cell level, these studies have identified the lymphoid tissues and the spleen as sites of highest persister concentration [34], have tried to address the replication dynamics of persisters' progenitors [6, 34], have provided insights in the inter-organ bacterial exchange during the gastrointestinal phase of infection [35], and have studied antibiotic-driven persistence in the context of cooperative virulence [36] and promotion of antibiotic resistance [37].

A later study by Rossi *et al.*, 2017 [38] used clinically-relevant concentrations of both a beta-lactam and a second-generation fluoroquinolone antibiotic later in the infection process (72 hours post-inoculation) to qualitatively characterise and compare the effect of the antibiotics on the within-host *Salmonella* dynamics, thus providing a blueprint for using murine infections with Isogenic Tagged Strains (ITS) to address questions on the effects of antibiotic therapy on bacterial dynamics *in vivo*.

Differences in the experimental design of these studies, including timing, dose, route of antibiotic administration, tissues examined and experimental techniques have unravelled different facets of the effects of antibiotic therapy on different tissues, as summarised in table 1.

Table 1: Review of *in vivo* studies on the effects of antibiotic treatment on *S.* Typhimurium dynamics.

A comparative summary of the methodology and conclusions reached in different *in vivo* studies investigating the role of antibiotic treatment on the within-host dynamics of *S.* Typhimurium.

Study	**Helaine *et al.*, 2014**	**Kaiser *et al.*, 2014**	**Claudi *et al.*, 2014**	**Diard *et al.*, 2014**	**Rossi *et al.*, 2017**	**Bakkeren *et al.*, 2019**
Strain of mice	C57 Bl6 and BALB/c	C57BL/6	BALB/c and 129/Sv	129 Sv/Ev	C57BL/6	129 Sv/Ev
Strain of *S.* Typhimurium	12023s	SB300, derivative of SL1344	SL1344	SB300, derivative of SL1344	SL1344	SL1344
Pre-treatment of mice with streptomycin	no	yes	yes	yes	no	yes
Route of bacterial inoculation	intraperitoneal	intraperitoneal	oral/ intravenous	intraperitoneal	intravenous	oral/intravenous
Inoculum Dose (CFU)	2×10^{10}	5×10^{7}	$4 \times 10^{2} - 2 \times 10^{3}$ / $10^{7} - 2 \times 10^{10}$	5×10^{7}	10^{3}	5×10^{7}/ 10^{3}
Route of antibiotic administration	oral	intraperitoneal	intraperitoneal	oral	intraperitoneal	intraperitoneal
Antibiotic used	enrofloxacin	ciprofloxacin	enrofloxacin	ciprofloxacin	ciprofloxacin, ampicillin	ciprofloxacin/ ceftriaxone
Onset of administration of first antibiotic dose (days post-inoculation)	1	1	3	2	3	2
Cumulative daily antibiotic dose (mg/kg)	10	124	5	240	ciprofloxacin: 40 ampicillin: 300	ciprofloxacin: 120 ceftriaxone: 60
Duration of antibiotic treatment (days)	5	10	4	1	4	3
Detection of persister bacteria	yes	yes	yes	yes	*not in the scope of the study*	yes
Sites of persistence	spleen, mesenteric lymph nodes (MLN)	caecal lymph node	spleen	caecal tissues	*not in the scope of the study*	liver, spleen
Replication status of persister bacteria	Non-replicating	Slow-replicating	Replicating, Moderately-replicating, Slow-replicating	*not in the scope of the study*	*not in the scope of the study*	*not in the scope of the study*
Study of relapse phase	no	no	no	yes	yes	yes
Experimental techniques	Fluorescent-based markers coupled with live imaging microscopy	1. Fluorescent-based markers coupled with live imaging microscopy 2. ITS coupled with real time quantitative PCR	Fluorescent-based markers coupled with live imaging microscopy	1. Plating and enumeration of bacteria from tissue samples 2. Fluorescence microscopy of stained tissue sections *ex vivo*	Isogenic tagged strains coupled with Illumina sequencing	Confocal microscopy of stained tissue sections ex vivo

Despite the growing interest in characterising the effect of antibiotic treatment on different tissues, quantitative approaches to infer and separately quantify unobserved processes such as bacterial replication, death, migration and phenotypic switch remain underrepresented. Additionally, it is now commonly accepted that non-replicating bacterial subpopulations emerge as a result of antibiotic-exposure. However, the effect of different antibiotic classes, the tissues of origin of phenotypic variants, and the time point of emergence of these non-growing subpopulations still remain ambiguous. Finally, how bacterial populations recover in different tissues following antimicrobial withdrawal and how non-growing antibiotic-recalcitrant bacteria regain their replicative capacity during the relapse phase of an infection are both questions directly relevant to our understanding of bacterial disease recrudescence underpinning chronic infections.

An important first step to address these knowledge gaps was taken by Rossi *et al.* in their ITS-based study of the comparative effects of ampicillin and ciprofloxacin on *S.* Typhimurium *in vivo* [38]. The novel contributions of the study included the use of both a beta-lactam and a fluoroquinolone antibiotic to directly compare their effects in the same experimental setup, the study of both the treatment and the relapse phase, the use of clinically relevant doses of antibiotics after the appearance of symptoms in line with the anticipated clinical response, instead of supramaximal early therapy, and data collection on 4 different organs involved in the systemic phase of infection, addressing not only intra- but also inter-organ dynamics. Finally, unlike previous studies carried at the single bacterial level, Rossi *et al.* used a bacterial population-level experimental technique (ITS) in a biological system with well-established heterogeneity in its dynamics [6, 34-35].

In this follow-up study, we complement the bacterial population-level outputs of this study by developing a family of mechanistic mathematical models to identify and quantify the experimentally unobserved processes of bacterial replication, death, inter-organ migration and phenotypic switch that collectively underpin the qualitative changes in the net bacterial number in different organs documented in Rossi *et al.*, 2017 [38]. We perform a simulation-based study to show that heterogeneities in bacterial phenotypes can be detectable from data collected at the level of the whole bacterial population. This methodological finding expands the scope of questions that can be addressed using well-established techniques such as ITS. Motivated by the well-documented emergence of a persister, antibiotic-recalcitrant bacterial subpopulation upon antibiotic administration (reviewed in [39]) we consider two models: (1) the single-

phenotype model (SP) assumes a bacterial population with uniform dynamics, with each biological process described by a single parameter representing the average rate at which the process occurs, and (2) the dual-phenotype model (DP) assumes that the observed output of changing bacterial load in tissues is shaped by two bacterial subpopulations with different dynamics *in vivo*: one is a replicating, antibiotic-sensitive subpopulation, and the other is a non-replicating, antibiotic-recalcitrant subpopulation [40]. By comparing how well the best model within each of these two classes of models can recapitulate the experimentally observed dynamics, we infer that at clinically-relevant doses ampicillin, but not ciprofloxacin, induces a non-growing antibiotic-recalcitrant bacterial subpopulation.

2. Methods

2.1. Experimental Dataset Structure

This is a mathematical modelling study using experimental data by Rossi *et al.*, 2017 [38] on the effect of ampicillin and ciprofloxacin on the within-host dynamics of wild-type *S.* Typhimurium in the murine host. Two groups of C57BL/6 mice were inoculated intravenously with an equiproportionate mix of 8 Isogenic Tagged Strains (ITS) of S. *Typhimurium* amounting a total of 1000 colony-forming units (CFU). The infections were allowed to develop for 72 hours, at which time a proportion of the mice from each group was culled, their organs harvested (either partially or in totality), homogenised and plated to determine the number of CFUs per organ/sample. Furthermore, genomic DNA was prepared from the recovered bacteria and these DNA samples were subjected to next generation sequencing (NGS) in order to determine the proportion at which each of the 8 ITS was present.

Of the remaining mice, group A was started with 300 mg/kg ampicillin and group C was put on a 40 mg/kg ciprofloxacin regimen intraperitoneally (i.p.) per day (maximum recommended dosage for veterinary treatment of small rodents) [41-42]. Antibiotic treatment was maintained for 96 hours; a proportion of mice was killed at 24 hour intervals to determine the per organ total CFU count and ITS composition. In total, data were collected at 4 equally spaced time points during the antibiotic treatment.

For the last phase of the study, the antibiotics were stopped and the infection was allowed to relapse for 54 hours in both groups. Data were collected at 30 and 54 hours post antibiotic withdrawal.

2.2. Conceptual Model Structure

The liver, spleen and mesenteric lymph nodes (MLN) are well-established reservoirs for *Salmonella* bacteria [11, 35], while bacteraemia is also a hallmark of systemic salmonellosis. On the basis of previous biological insight and prior modelling attempts, and acknowledging that the enteric-systemic interface has not been extensively studied in tandem, we first considered a general compartmental model allowing all possible connections between the key

organs for which data were available, and with a single-phenotype bacterial population characterised by homogeneous dynamics (Figure 1). The parameters governing the transitions in the model, and mapping to the biological processes *in vivo* are described in table 2.

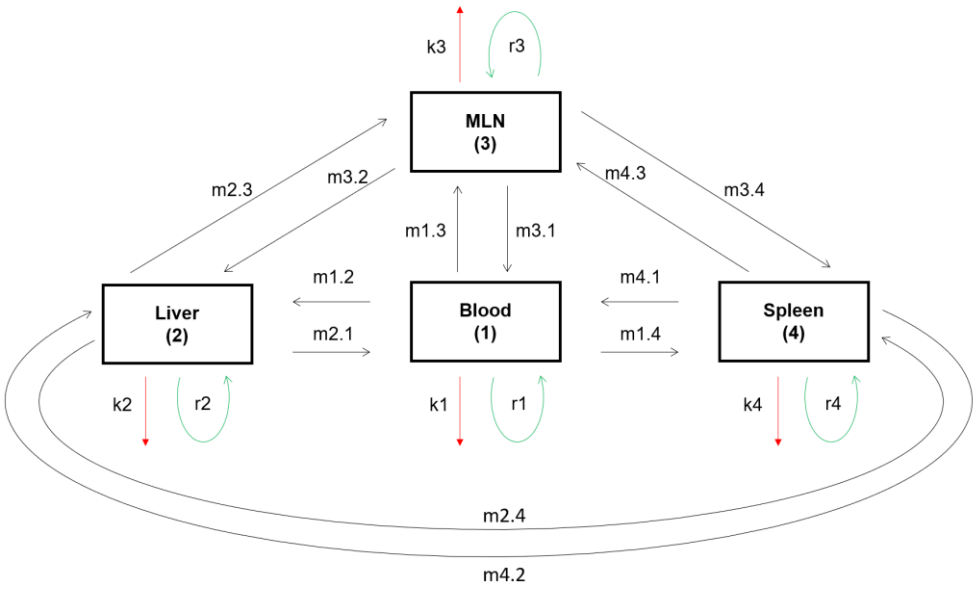

Figure 1: Generalised single-phenotype model with free inter-organ bacterial migration between the blood, liver, MLN and spleen, and with intra-organ bacterial death and replication in the all organs.

As an extension to the single-phenotype model and given the prolonged exposure to antibiotic-induced stressed, we proceeded to formulate a dual-phenotype model (Figure 2). This model assumes the emergence of a bacterial subpopulation which is non-replicating and survives antibiotic treatment (Figure 2).

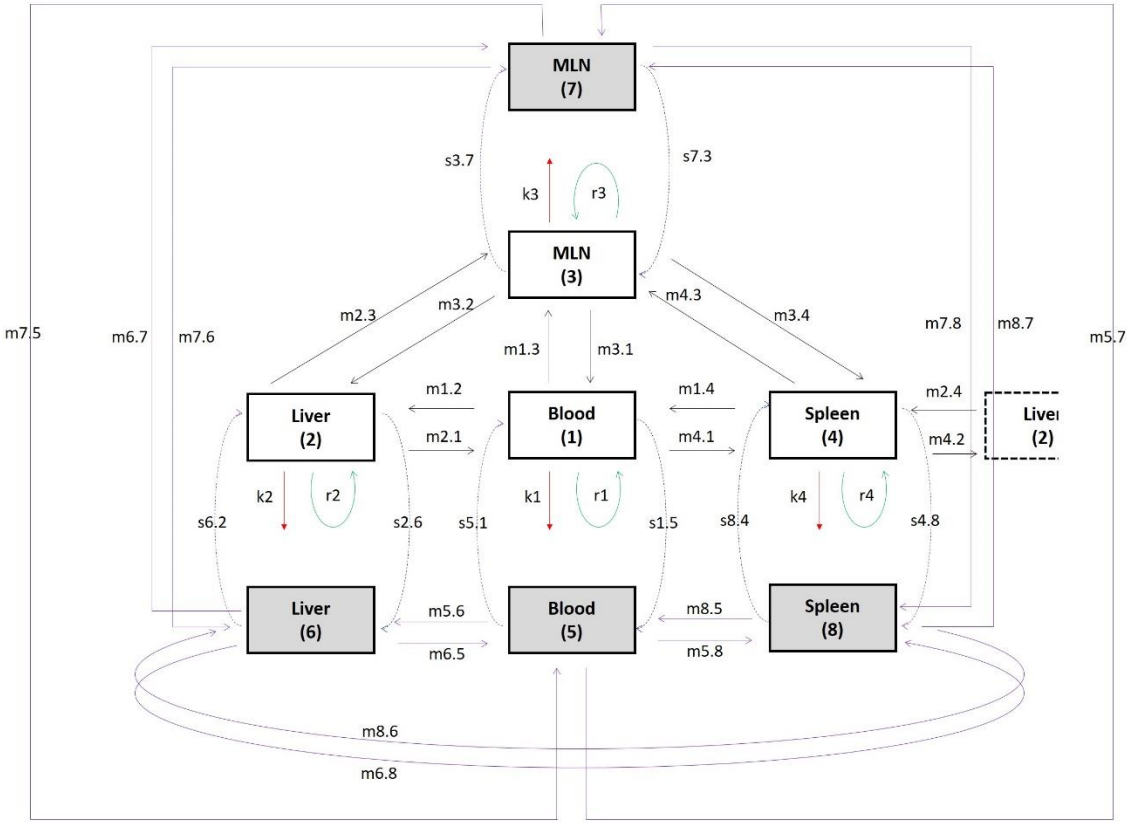

Figure 2: The dual-phenotype (DP) model encompasses a phenotypic switch from replicating bacteria susceptible to killing to non-growing, antibiotic-recalcitrant subpopulations in the liver, spleen and MLN, highlighted in grey.

	Parameter name	Description
Inter-organ migration (P1)	m1.2	Bacterial migration from the blood to the liver
	m1.3	Bacterial migration from the blood to the MLN
	m1.4	Bacterial migration from the blood to the spleen
	m2.1	Bacterial migration from the liver to the blood
	m3.1	Bacterial migration from the MLN to the blood
	m4.1	Bacterial migration from the spleen to the blood
	m2.3	Bacterial migration from the liver to the MLN
	m2.4	Bacterial migration from the liver to the spleen
	m3.2	Bacterial migration from the MLN to the liver
	m4.2	Bacterial migration from the spleen to the liver
	m3.4	Bacterial migration from the MLN to the spleen
	m4.3	Bacterial migration from the spleen to the MLN
Inter-organ migration (P2)	m5.6	Bacterial migration from the blood to the liver
	m5.7	Bacterial migration from the blood to the MLN
	m5.8	Bacterial migration from the blood to the spleen
	m6.5	Bacterial migration from the liver to the blood
	m7.5	Bacterial migration from the MLN to the blood
	m8.5	Bacterial migration from the spleen to the blood
	m6.7	Bacterial migration from the liver to the MLN
	m6.8	Bacterial migration from the liver to the spleen
	m7.6	Bacterial migration from the MLN to the liver
	m8.6	Bacterial migration from the spleen to the liver
	m7.8	Bacterial migration from the MLN to the spleen
	m8.7	Bacterial migration from the spleen to the MLN

Intra-organ dynamics (P1)	k1	Bacterial death in the blood
	k2	Bacterial death in the liver
	k3	Bacterial death in the MLN
	k4	Bacterial death in the spleen
	r1	Bacterial replication in the blood
	r2	Bacterial replication in the liver
	r3	Bacterial replication in the MLN
	r4	Bacterial replication in the spleen
Phenotypic switch (between P1 and P2)	s2.6	Switch from P1 to P2 in the liver
	s6.2	Switch from P2 to P1 in the liver
	s3.7	Switch from P1 to P2 in the MLN
	s7.3	Switch from P2 to P1 in the MLN
	s4.8	Switch from P1 to P2 in the spleen
	s8.4	Switch from P2 to P1 in the spleen
	s1.5	Switch from P1 to P2 in the blood
	s5.1	Switch from P2 to P1 in the blood

Table 2: Description of parameters used in the mechanistic models

P1 refers to the growing, antibiotic-sensitive bacteria and P2 refers to the non-growing, antibiotic-recalcitrant bacteria.

2.3. The modelling framework

Mathematically, these models (Figures 1 and 2) are translated into multivariate continuous-time Markovian processes [43], with stochastic variables each representing the number of bacteria in the blood, liver, spleen and MLNs (observed experimental output). The dynamics of such processes, in particular the probability that the system is at a given state at any particular time point, can be summarised by the forward Kolmogorov equation, which describes this probability in terms of the contribution of each of the biological processes included in the mechanistic model (bacterial replication, killing, migration and phenotypic switch). In this case, the state refers to a vector consisting of the number of bacteria in all 4 locations at the time point of interest. Transitions between different states, i.e. any change in the number of bacteria in any of the tissues of interest over time, are driven by dynamical processes quantified by parameters, reflecting the rate of development of unobserved bacterial dynamics in time.

2.3.1. Summary statistics for cross-distribution comparison

For a multivariate stochastic system, the overarching forward Kolmogorov equation becomes analytically intractable for multi-compartmental systems with numerous parameters. To avoid the step of solving the probability density function characterising the multivariate bacterial

distribution, we use summary statistics to capture the necessary features of interest. Our models only incorporate zero-order dynamics, thus the first- (mean numbers of bacteria in each organ) and second-order (variance-covariance matrix of bacterial numbers in all organs) moments suffice to describe the distribution [44].

2.3.2. Divergence minimisation parameter inference framework

Here, we solve the mathematical models retrospectively using experimentally measured outputs (numbers of bacteria per organ) with the aim to estimate the values of unobserved processes, which correspond to parameters characterising bacterial replication, death, migration and switching to a non-growing phenotype. To achieve this, we use a likelihood-free inference framework, which overrides the problem of intractability. As the multivariate distribution is characterised by a set of first- and second- order moments, it is possible to explore parameter value combinations with the aim of reaching a distribution that approximates the experimentally observed bacterial distribution as closely as possible. This is achieved by minimising a quantity (cost function) that cumulatively expresses the divergences between each experimentally-observed and predicted pair of moments [44]. In this case we choose the Kullback-Leibler divergence as the cost function to be minimised.

Parameter inference was performed using the freely available SPEEDI.R package [45] and the Nelder & Mead [46] optimisation algorithm.

2.2.3. Parametric bootstrap for quantification of inference precision and assessment of model goodness-of-fit

Goodness-of-fit is a measure of how well a given model captures the experimental data. Here, we use a parametric bootstrap approach to assess model goodness-of-fit. Using minimum-divergence moments-based inference, we identify the set of parameters that correspond to first- and second-order moments and yield the smallest divergence from the observed moments. This set of moments is referred to as the predicted moments and the corresponding parameter set as the predicted parameters.

Using the predicted parameters, we simulate 500 samples of size emulating the number of observations (10 mice x 8 ITS = 80 or 5 mice x 8 ITS = 40) per time point in the experimental dataset. For each simulated sample, we calculate the corresponding moments and compare each set of moments with the predicted moments to obtain a divergence value. We refer to those moments as simulated moments. If each of the experimental moments fall into their respective distribution of simulated moments, the goodness-of-fit is adequate and the model can be accepted as plausible.

We, then, use the simulated moments to anew infer the range of parameter values, which provide the confidence intervals for our original parameter estimates, and thus serve as a measure of the inference precision.

3. Results

3.1. Simulation study for the detection of heterogeneity in ITS data

Using infections with mixed inocula comprising ITS it is possible to infer the rates at which inter- and intra-organ dynamics of infection change over time. However, it has not hitherto been shown whether data from ITS-based studies can be used to address questions about heterogeneity in within-host dynamics. Here, we are interested in comparing the performance of a SP model assuming a single bacterial population with uniform dynamics, and that of a DP model assuming two bacterial subpopulations with different dynamics, described in section 2.2.

We performed a simulation-based study to investigate whether bacterial populations with uniform replication and death dynamics could be reliably distinguished from bacterial populations composed of both a growing, antibiotic-sensitive subpopulation and a non-growing, antibiotic-recalcitrant subpopulation, by applying mechanistic models to simulated data from synthetic ITS-based "experiments".

We simulated 10 synthetic datasets with different parameter sets from the dual phenotype DP-model. We then applied both the SP- and DP-models to the 10 synthetic datasets to obtain a best parameter estimate, and as per 2.2.3, we used a parametric bootstrap approach to generate 500 bootstrapped samples for each of the 10 synthetic datasets under the two models. We finally performed a pairwise comparison of their goodness-of-fit.

We used two tools to evaluate the goodness-of-fit of the SP- and DP- models to the synthetic datasets. The first was the pairwise comparison of the KL divergences; a lower divergence indicates a better fit between the model and the synthetic data. The second tool was the pairwise comparison of the similarity between each synthetic dataset and its bootstrapped samples when the DP- or SP- model was used respectively. To this end, for each of the two models we obtained the mean value and standard deviation of each moment for the 500 bootstrapped samples and calculated the number of standard deviations between each true moment value and the mean value from the bootstrapped samples.

For all 10 synthetic datasets simulated from the DP-model, the DP-model gave consistently lower Kullback-Leibler (KL) divergence values by two orders of magnitude, compared to the SP-model (shown in Table 3). When applied to DP-data, the bootstrapped samples from the DP-model were more similar to the original synthetic data than bootstrapped samples from the SP-model (Figure 3).

Overall, this simulation study shows that phenotypic heterogeneity at the level of two subpopulations is detectable from ITS-based data collected at the level of the entire bacterial population.

Table 3: Pairwise comparison of KL-divergence values from DP- and SP- model fitting to synthetic datasets simulated from the DP-model.

Synthetic dataset index	KL divergence from DP- model	KL divergence from SP- model
1	0.0031	0.55
2	0.0053	1.38
3	0.0041	0.88
4	0.0013	0.20
5	0.0026	1.17
6	0.0045	0.47
7	0.0017	0.46
8	0.0045	0.45
9	0.0012	0.92
10	0.0046	1.16

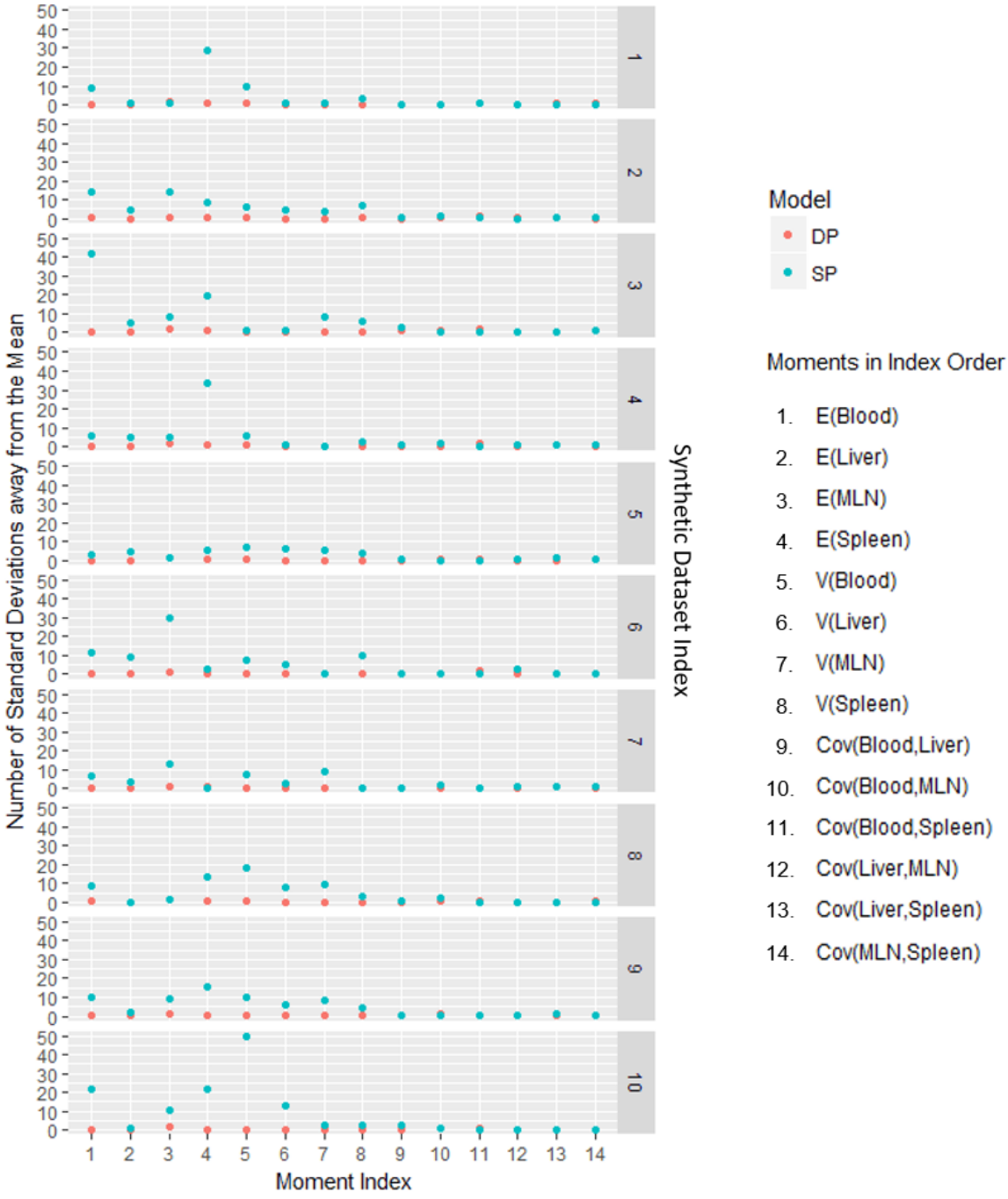

Figure 3: Comparison of SP- and DP- model performance on synthetic data simulated from the DP-model. Each of the horizontal panels (1-10) represents the fit between one synthetic dataset and the SP- and DP-models in blue and red respectively. The blue and red dots represent the number of standard deviations between the moments of the virtual dataset and the mean value of 500 bootstrapped datasets generated from the best parameter set in the SP and DP model respectively. The moment indices in the x-axis refer to the 14 means, variances and covariances used as summary statistics of the ITS distributions in the 4 organs. The number of standard deviations is always near-zero when the DP-model is applied (red), while consistently higher when the SP- model is applied (blue).

3.2. Model Selection

First, we identified the best-fitting, most parsimonious model from the family of single-phenotype (SP) models, whose structure is shown in Figure 1. Starting from a fully parameterised model (12 parameters), we fitted sequentially simpler models (nested models) to data from ampicillin- and ciprofloxacin treated mice day-by-day for 4 days of total treatment and 2 days post-treatment. For each treatment group, we used the ITS counts per organ at 72 hours post-inoculation as the starting point and the respective ITS counts at 24 hours post-treatment to mark the end of the first day of the antibiotic regimen, and inferred the best parameter estimate set, as detailed in 2.5.1. We repeated the same inference process to estimate the parameter values for each time interval separately, totalling 4 time intervals during antibiotic treatment and 2 during the relapse phase.

We repeated the same process for the family of DP models, whose structure is shown in Figure 2. The best-fitting models for the SP and DP family of models are comparatively summarised for each time interval, in the ampicillin- and ciprofloxacin-treated groups. Note that where the DP model offers no improvement in fitting the experimental data, the best DP model converges to the best-fitting SP model (Tables 4 and 5 respectively).

Table 4: Comparative summary of best-fitting SP- and DP- models in the ampicillin-treated mice

Model	Treatment Group	Time Interval (days after start of treatment)	Parameters Estimated	Number of Parameters Estimated	KL divergence
SP	Ampicillin	1	k1,k2,k3,k4,r2,r3,r4,m4.2	8	0.66
DP	Ampicillin	1	k1,k2,k3,k4,r2,r3,r4,m4.2	8	0.63
SP	Ampicillin	2	k1,k2,k3,k4,r2,r3, r4	7	0.98
DP	Ampicillin	2	k1,k2,k3,k4,r2,r3, r4	7	0.93
SP	Ampicillin	3	k1,k2,k3,k4,r2r3,r4	7	1.60
DP	Ampicillin	3	k1,k2,k3,k4,r2,r3,r4,m4.8,m8.6	10	0.56
SP	Ampicillin	4	k1,k2,k3,k4,r3,r4, m1.4	7	0.50
DP	Ampicillin	4	k1,k2,k3,k4,r1,r2,r3,r4,m3.7,m4.8	10	0.49

SP	Ampicillin	5	k2,k3,k4,r1,r2,r3,r4	8	0.58
DP	Ampicillin	5	k2,k6,k7,k8,r1,r2,r6,r7,r8	9	0.12
SP	Ampicillin	6	k1,k2,k3,k4,r1,r2,r3,r4	8	0.73
DP	Ampicillin	6	k1,k2,k6,k7,k8,r1,r2,r6,r7,r8	10	0.39

406

407

408 **Table 5: Comparative summary of best-fitting SP- and DP- models in the ciprofloxacin-treated mice**

409

Model	Treatment Group	Time Interval (hours after start of treatment)	Parameters Estimated	Number of Parameters Estimated	KL divergence
SP	Ciprofloxacin	0-24	k1,k2,k3,k4,r1,r2,r3,r4	8	0.06
DP	Ciprofloxacin	0-24	k2,k4, r2,r4,m3.7,m1.2	6	0.40
SP	Ciprofloxacin	24-48	k1,k2,k3,k4,r1,r2,r3,r4,m2.4	8	2.91
DP	Ciprofloxacin	24-48	k1,k2,k4,r2,r4,m2.4,m3.7,m4.8, m8.6	8	3.40
SP	Ciprofloxacin	48-72	k1,k2,k3,k4,r1,r2,r3,r4,m2.4	9	0.25
DP	Ciprofloxacin	48-72	k1,k2,k3,k4,r1,r2,r3,r4,m1.4,m4.8, m2.6,m8.4,m6.2,m7.3	14	0.33
SP	Ciprofloxacin	72-96	k2,k3,k4,r1,r2,r3,r4	7	0.14
DP	Ciprofloxacin	72-96	k2,k3,k4, r1,r2,r3,r4,m4.8,m8.4, m6.2	10	0.19
SP	Ciprofloxacin	96-126	k2,k3,k4,r1,r2,r3,r4	7	0.54
DP	Ciprofloxacin	96-126	k2,k3,k4,k5,k7,k8,r2,r3,r4,r5,r7,r8, m6.8	13	0.85
SP	Ciprofloxacin	126-140	k1,k2,k3,k4,r1,r2,r3,r4,m2.4	9	0.38
DP	Ciprofloxacin	126-140	k1,k2,k3,k4,r1,r2,r3,r4,m2.4	9	0.38

410

411 Having identified the best-fitting model from each model family for each of the 6 time intervals
412 considered in each of the 2 treatment groups, we then assessed whether the divergence of the

best predicted model from the experimental data can be recapitulated by bootstrapped datasets simulated from the best parameter set corresponding to the best fitting models. Given that the DP model family is more complex than the SP model family, we chose the best-fitting DP model as superior to the best-fitting SP model only if bootstrapped data from the former were consistently more similar to the experimentally observed data than synthetic data from the SP model.

To quantify the similarity between the experimentally observed and bootstrapped data produced from either the best-fitting SP or the best-fitting DP models, we calculated the first- and second-order moments for each of the 500 bootstrapped datasets produced from each of the best-fitting models per time interval per treatment group, followed by the mean and standard deviation for each of those moments. As illustrated in Figure 4, we then calculated in standard deviations the distance between the moments from the experimentally observed data and the mean values for the moments of the bootstrapped samples, similarly to 3.1.

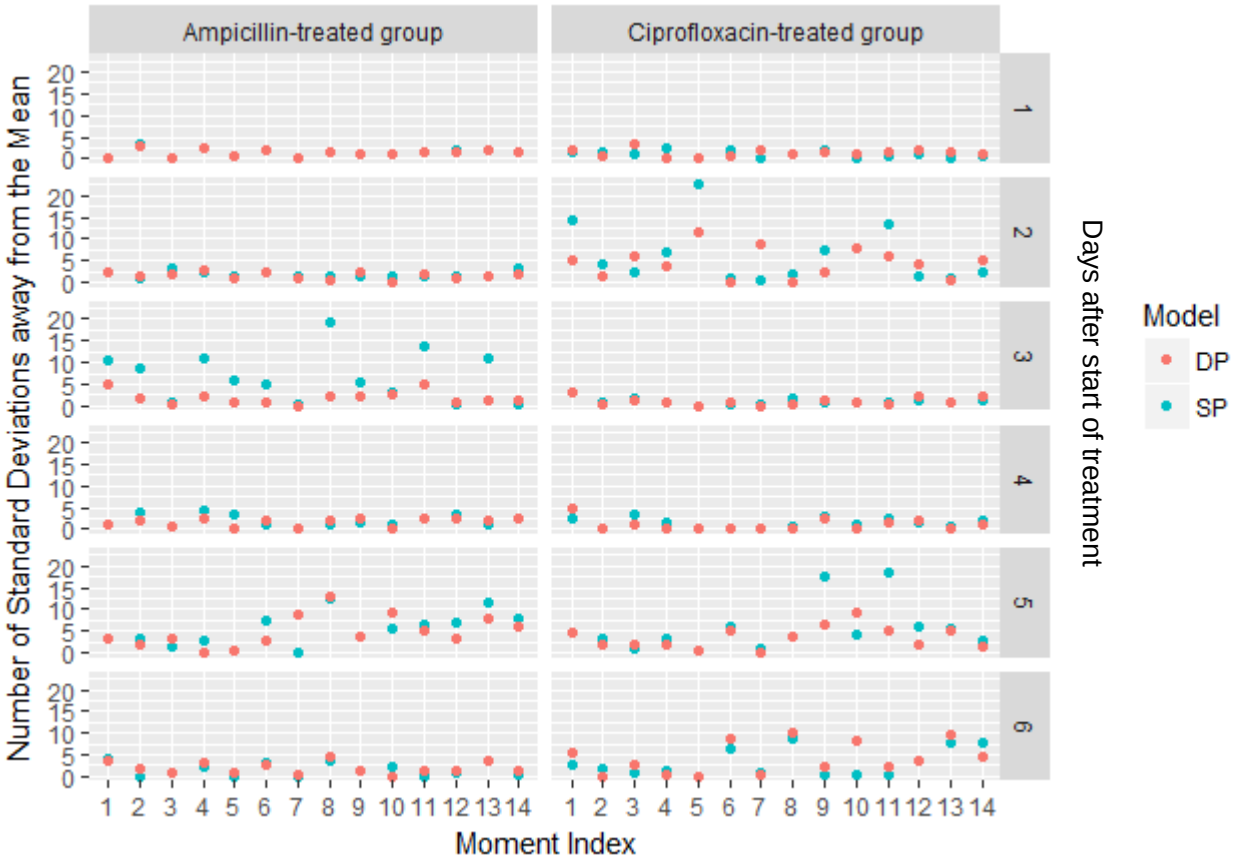

Figure 4: Comparison of SP and DP model performance assessing the relationship between model-based simulations and observed experimental values

The blue and red dots represent the number of standard deviations between the experimentally observed moments and the mean value of 500 bootstrapped datasets generated from the best parameter set in the SP and DP model respectively, for each time point. The indices in the x-axis refer to the 14 means, variances and covariances used as summary statistics of the ITS distributions in the 4 organs. The enumeration of the horizontal panels (1-6) refers to the number of days after the start of antibiotic treatment. In ampicillin-treated mice, improvement in the model fit with the DP model is shown by an overall reduction of the number of standard deviations between the experimentally observed moments and the mean value of 500 parametric datasets, especially during days 2, 3 and 5. In ciprofloxacin-treated mice, there is no consistent improvement when the DP model is applied.

3.3. SP and DP model comparison in ampicillin-treated mice

We applied the SP model, described in section 2.2., to the dataset from the ampicillin-treated group. Upon obtaining the best parameter estimates for each time interval, we simulated 500 bootstrapped datasets to obtain a distribution of values for each of the moments. We expected that in a well-fitting model, the experimentally observed moments would fall within the distribution of bootstrapped moments. Figure 5 summarises the results of the fit of the DP- and SP- model to the experimental data, showing that the DP-model improves the fit of the model to the experimental data, on days 3-5 after the start of treatment.

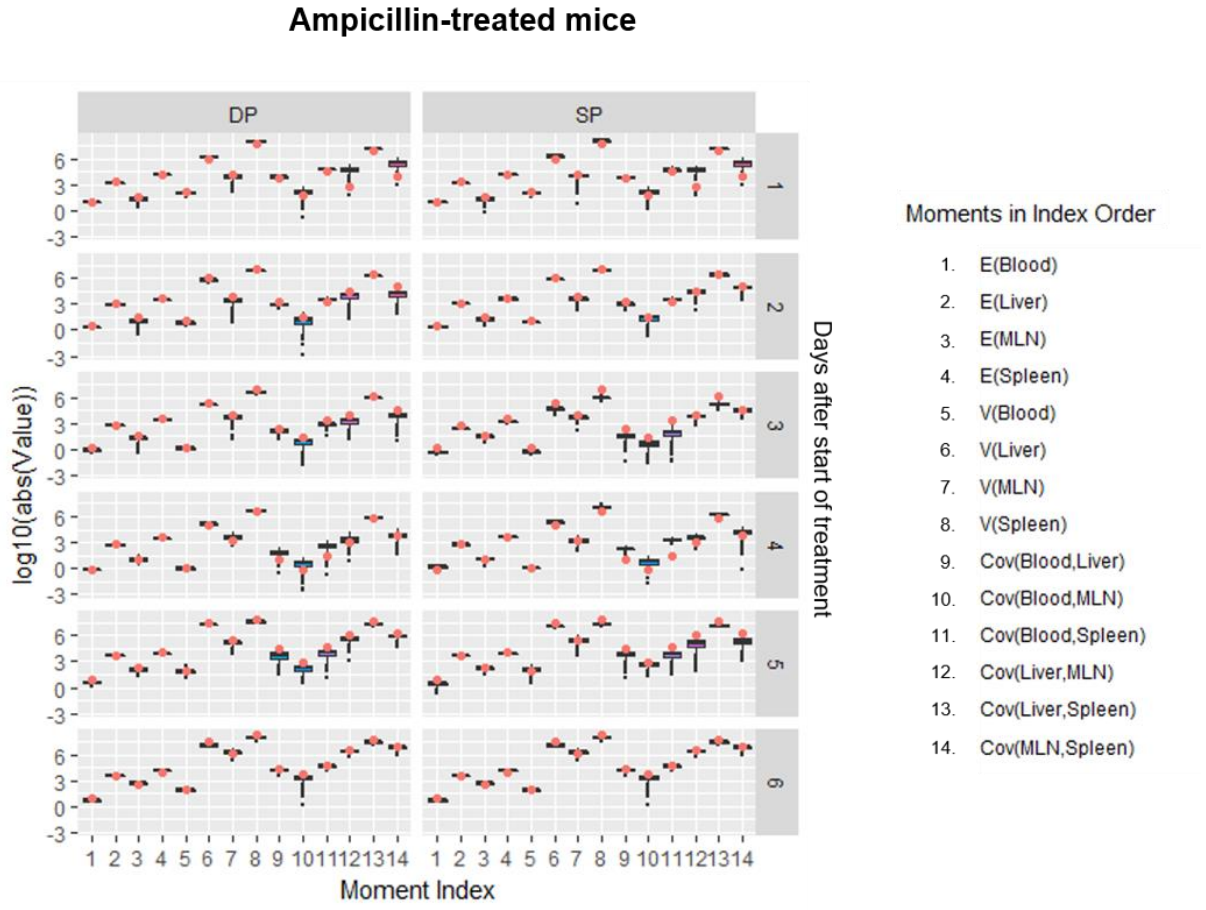

Figure 5: Comparison between the fit of the SP- and DP- models to the experimental data

Each of the boxplots captures the distribution of 500 bootstrapped values for each of the 14 first- and second-order moments, while each red dot represents the value of the same moment from the experimentally observed data. Improvements can be seen in moments with indices 8, 9, 10, 11 and 14 on day 3, moments with indices 1, 6, 8, 9, 10, 11 and 13 on day 4, and moments with indices 6, 8, 12 and 14 on day 5. The improvement mostly concerns the variances (indices 4-8) and covariances (indices 8-14).

3.4. SP model-fit in ciprofloxacin-treated mice

We then applied the SP-model, described in section 2.2., to the dataset from the ciprofloxacin-treated group and obtained a distribution of values for each of the moments, as in 3.2. Here, we show that throughout the treatment and relapse phase, the experimentally observed moments can be recapitulated by simulations from the SP-model given the best set of parameter estimates (Figure 6).

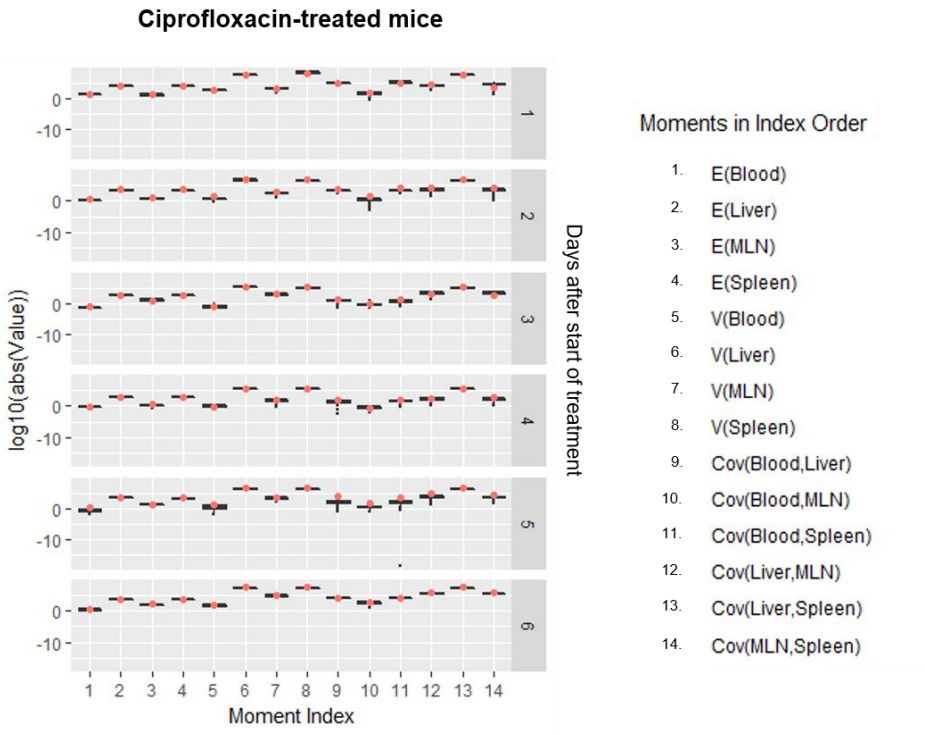

Figure 6: Experimental moments in relation to moments from synthetic data using the best-fitting SP model

3.5. Intra-organ dynamics during treatment phase

Our models predict that ampicillin and ciprofloxacin exert different effects on intra-organ bacterial dynamics in terms of their bactericidal and bacteriostatic effects (Figure 7). While in ciprofloxacin-treated mice, bacterial replication occurs throughout the duration of treatment in all four organs, ampicillin suppresses bacterial replication, particularly in the blood and in the late phase of treatment in the spleen and MLN. The occasionally wide confidence intervals in our estimates are explained by the correlation between replication and killing rates, as shown in by the narrow ellipses in Figure 8.

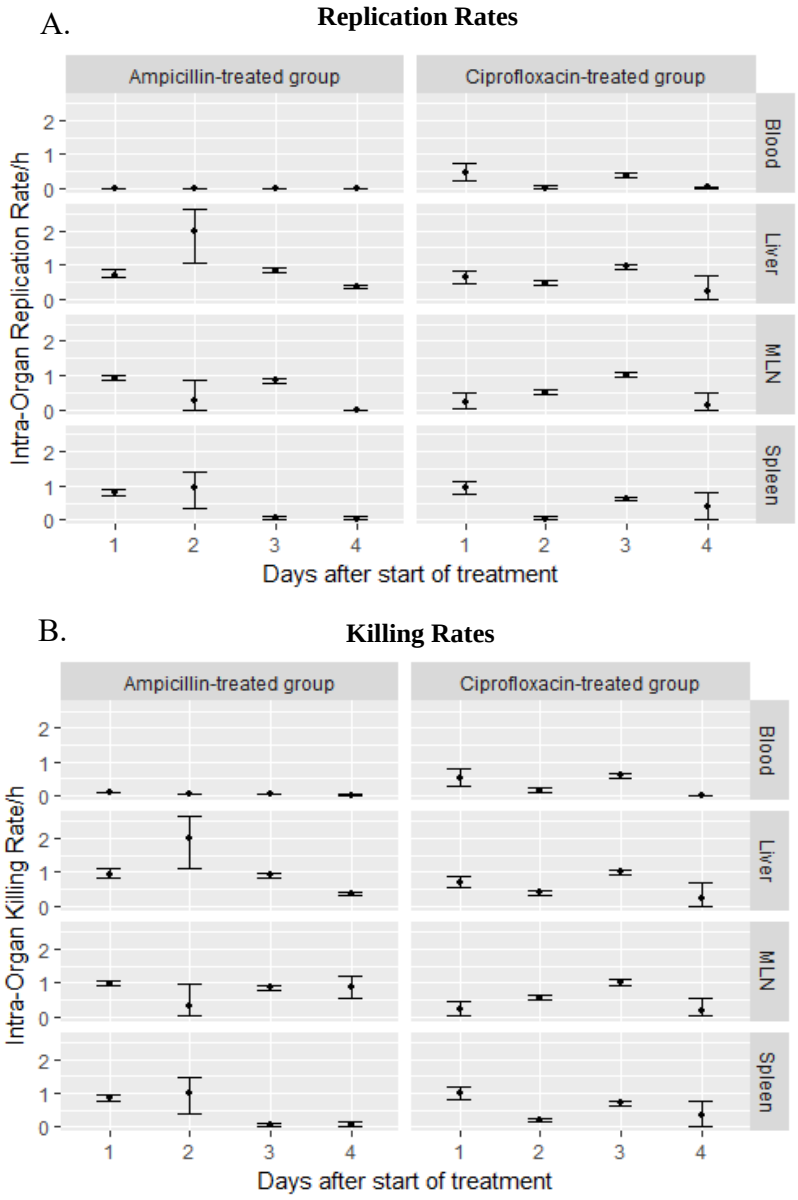

Figure 7: 95% confidence intervals of intra-organ replication and killing rates estimated from 500 parametric bootstrapped samples from the best parameter estimates

Panel A comparatively shows the replication rates for ampicillin-treated and ciprofloxacin-treated groups, while panel B shows the killing rates for the two groups. The dots represent the mean values across 500 parametric bootstrapped samples from the best parameter estimates, while the bars represent the lower and upper boundaries of the 95% confidence intervals. The cidal activity in ciprofloxacin-treated mice culminates after 3 days of treatment, while the static effects of ampicillin peak after 4 days of treatment.

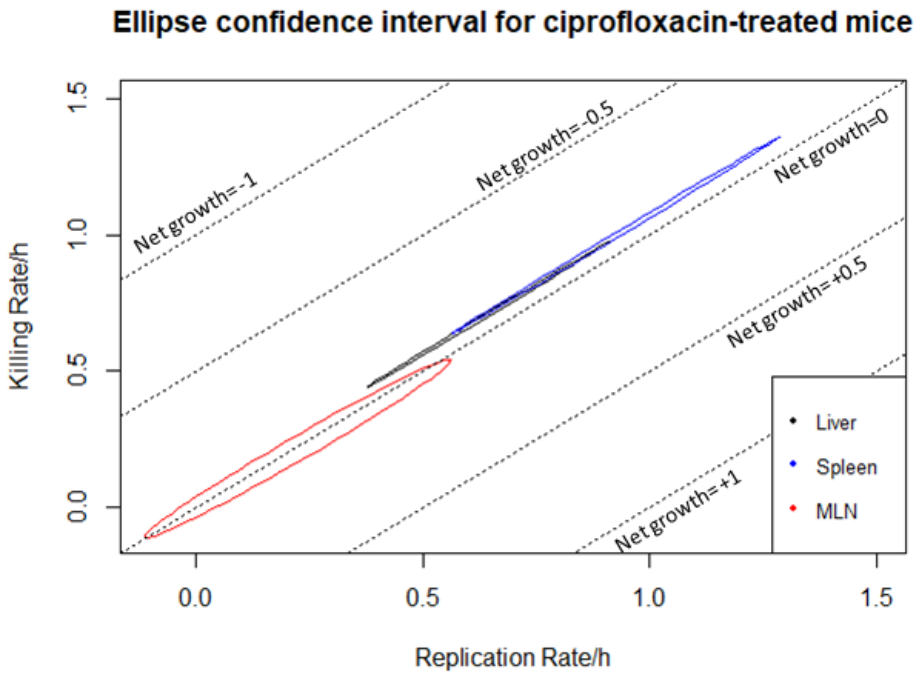

Figure 8: Bivariate 95% confidence intervals of intra-organ replication and killing rates (500 bootstrapped samples) for ciprofloxacin-treated mice 1 day after treatment.

The black, blue and red ellipses illustrate the bivariate 95% confidence interval for replication and killing rate in the liver, spleen and MLN respectively during day 3 after the start of ciprofloxacin treatment. The large length of the major axis of the ellipse represents the high correlation between replication and killing parameter estimates, which accounts for the large confidence intervals seen in Figure 7. Diagonal grid lines indicate net growth rates (replication rate-killing rate). In the liver and spleen, cidal effects are stronger leading to a negative net growth rate, while net growth in the MLN is close to 0.

3.6. Non-growing subpopulations recalcitrant to antibiotic therapy in ampicillin-treated mice

In ampicillin-treated mice, the best-fitting DP-model predicts the emergence of a non-growing, antibiotic-recalcitrant bacterial subpopulation. Our inference shows that this bacterial subpopulation emerges 48 hours after treatment with ampicillin at varying proportions in different organs and over time. By 72 hours of treatment, non-growing antibiotic-recalcitrant bacteria originating from the spleen have migrated to the liver. By 96 hours, the entirety of the bacterial population in the MLN and spleen have switched to the non-growing, antibiotic-insensitive phenotype, as summarised in Figure 9.

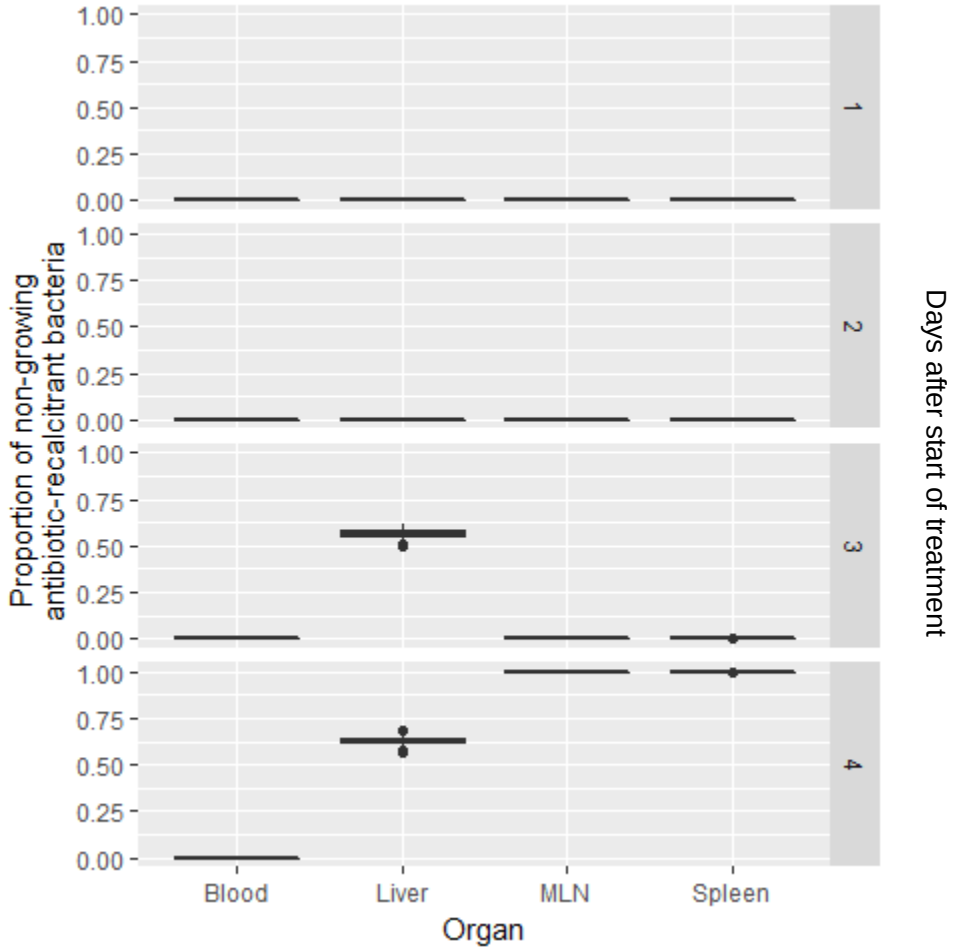

Figure 9: Proportion of persister bacteria in the blood, liver, MLN and spleen during ampicillin-treatment The confidence intervals for the proportion of persister bacteria are expressed as a fraction of total bacterial number in the liver, MLN and spleen (500 bootstrapped samples).

3.7. Dynamics in the relapse phase

Following withdrawal of the 4-days of antibiotic treatment, bacterial infection relapses in both ampicillin- and ciprofloxacin-treated groups, with positive net growth rates in the first 30 hours post-withdrawal. In the ampicillin-treated group, the progeny of the growing subpopulation has a different net growth to that of the non-growing, antibiotic-recalcitrant one in the liver (Liver (P)), MLN (MLN (P)) and spleen (Spleen (P)), shown in figure 10.

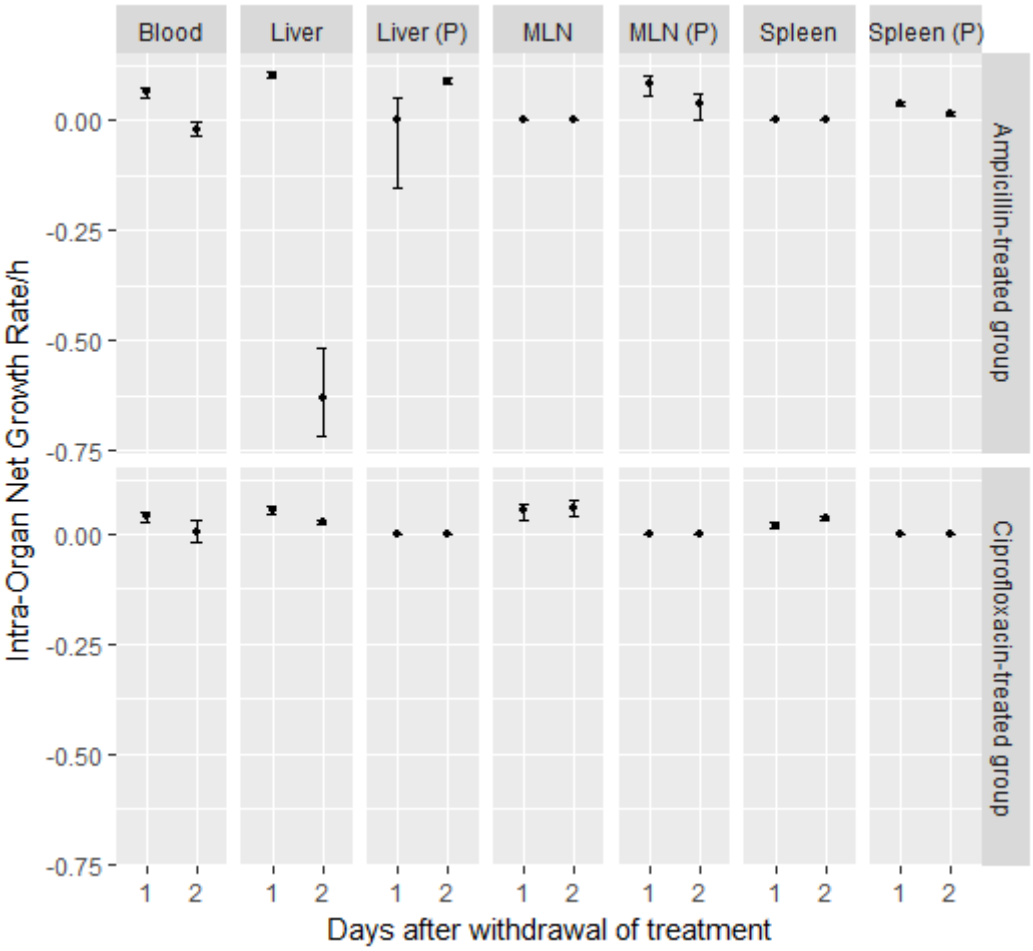

Figure 10: 95% confidence intervals of net growth rates (replication - killing rate) during relapse, estimated from parametric bootstrapped samples based on the best set of parameter estimates

In the ciprofloxacin-treated group with the predicted single bacterial phenotype, the relapse phase is characterised by positive net growth across all organs, with small fluctuations during the 2 days post ciprofloxacin withdrawal. In the ampicillin-treated group, the comparison between the net growth rates for the progenitors of the previously non-growing subpopulation with those of their previously growing counterparts in the liver shows that the former are consistently higher than the latter. Following bacterial relapse, all organs are repopulated by progenitors of the previously non-growing, antibiotic-recalcitrant subpopulation.

To understand what drives the extinction of the previously growing antibiotic-sensitive population in the liver of ampicillin-treated mice, we compare the killing and replication rates between the progeny of the previously growing and the persister population (Figure 11).

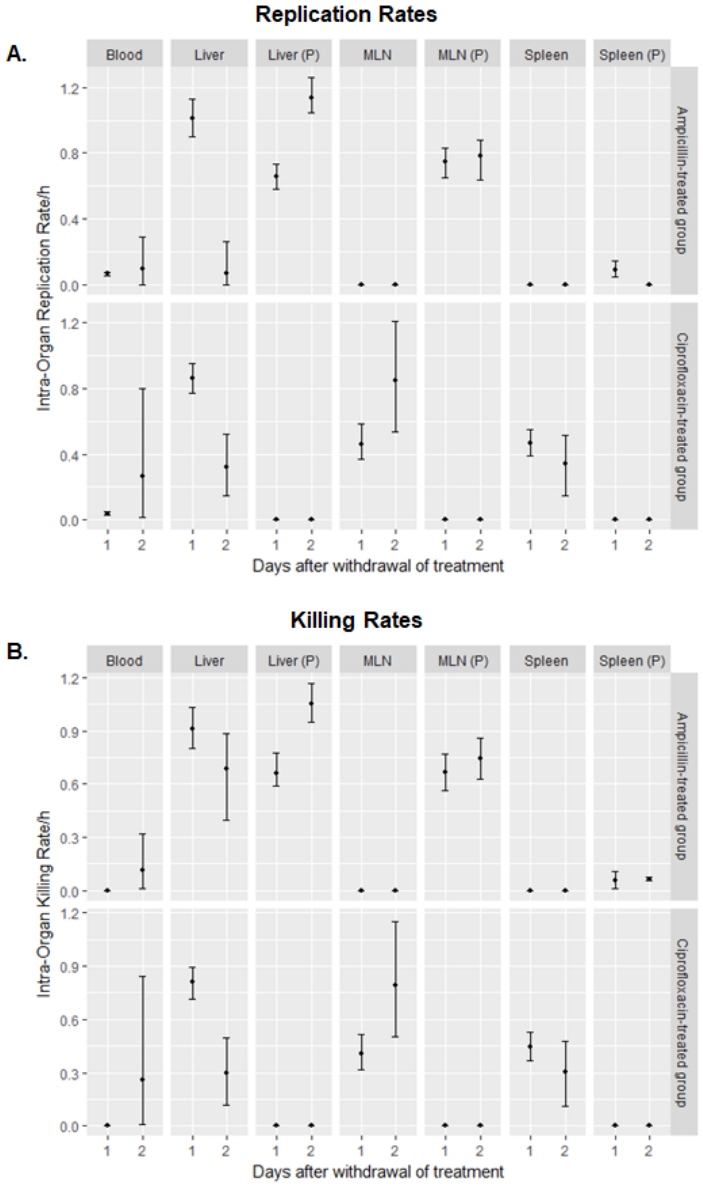

Figure 11: 95% confidence intervals of intra-organ replication and killing rates estimated from 500 parametric bootstrapped samples from the best parameter estimates during the relapse phase

Panel A comparatively shows the replication rates for ampicillin-treated and ciprofloxacin-treated groups, while panel B shows the killing rates for the two groups. The dots represent the mean values across 500 parametric bootstrapped samples from the best parameter estimates, while the bars represent the lower and upper boundaries of the 95% confidence intervals. In the ampicillin-treated mice, progenitors of the non-growing antibiotic-recalcitrant bacterial reservoir in the liver (Liver (P)) replicate at a higher rate on average compared to the progenitors of their previously growing counterparts (Liver).

4. Discussion

In the present data-based modelling study, we set out to quantify the effects of ciprofloxacin and ampicillin on the *in vivo* dynamics of *S.* Typhimurium in the murine host. Complementing previous studies, this is a mathematical modelling study based on data collected at the level of the bacterial population, using a virulent SL1344 *Salmonella* strain in C57BL/6 immunocompetent mice that have not been pre-treated with antibiotics. We used data from mouse infections with two different classes of antibiotics, one beta-lactam and one fluoroquinolone to directly compare their *in vivo* effects on the bacterial dynamics in an intravenous infection of wild-type mice, closely mimicking the systemic phase of non-typhoidal salmonellosis [38].

The inferential capacity of our mechanistic models is dependent on quantitative signals present in the experimental data collected by Rossi *et al.* [38], i.e. changes in the mean number of ITS copies per organ during time, their variance and their joint variability across all organs (covariance). Mathematical models can make use of the direction, magnitude and collective effect of these changes to maximise the insight provided by experimental data, especially if the changes in the mean numbers, which constitute the primary tool for qualitative inference, are not strikingly dissimilar. Our simulation study shows that when a single-phenotype model is applied to data from a dual-phenotype system, there is consistent misestimation of the variances across all 10 synthetic datasets. In our experimental data, the ill fit of the SP-model during days 3 and 4 of treatment mainly concerns variances and covariances. It, thus, appears that the quantitative signal allowing us to carry out this inference lies in the second-order moments (variances, covariances) of the ITS distribution in the organs.

As a proof-of-concept, we first conducted a simulation-based study to show that mechanistic models applied to ITS-based data can distinguish between bacterial populations with uniform and heterogeneous dynamics. Then, we fit a both a SP- and a DP- model to data from ampicillin- and ciprofloxacin-treated mice. Our best-fitting models suggest that a SP population can explain the dynamics in ciprofloxacin-treated mice, while the dynamics in ampicillin-treated mice are further complicated by bacterial phenotypic heterogeneity, best captured by the DP model with a non-growing, antibiotic-recalcitrant bacterial subpopulation. Inferences made regarding the rates at which these dynamics develop over time indicate that while ciprofloxacin acts predominantly via cidal mechanisms, ampicillin has mixed

bacteriostatic and bactericidal effects [47]. At the end of ampicillin treatment, surviving bacteria in the MLN and spleen have adopted a non-replicating, antibiotic-recalcitrant phenotype; in contrast, the vast majority of surviving bacteria in the ciprofloxacin-treated group are of the growing, antibiotic-sensitive phenotype. Following antibiotic withdrawal, bacteria relapse in both the ampicillin- and ciprofloxacin-treated groups of mice. In ciprofloxacin-treated mice, growth rate in the blood, liver and spleen is higher on day 1 post- antibiotic withdrawal and, subsequently decreases. In ampicillin-treated mice, the liver, spleen and MLN are repopulated by progenitors of the non-growing antibiotic-recalcitrant bacteria.

These results can be discussed in the context of previous experimental studies using alternative observational techniques, including non-phenotypic marker-based techniques [35-36, 46] fluorescence dilution [34] and peak-to-trough ratio [23]. An *in vitro* study by Ghooi and Thatte [26] showed that beta-lactam antibiotics, such as ampicillin, act as both bacteriostatic and bactericidal agents, due to their concomitant action on bacterial cell wall synthesis inhibition preventing bacterial replication, and their action on autolysins inducing bacterial death respectively. McCall *et al.* [5] introduced the phenomenon of antibiotic-induced stasis to explain the emergence of a slow- or non-growing bacterial population as a result of exposure to antibiotics with bacteriostatic effects and proceeded to show that this population cannot be killed by the same antibiotic class. The inferences made by our best-fitting DP model based on data from ampicillin-treated mice aligns with these documented *in vitro* effects of ampicillin on bacterial growth, as we estimated both strong bacteriostatic effects in the blood and the organs after 48 hours of treatment, and the emergence of a non-growing, antibiotic-recalcitrant subpopulation in organs where persisters have previously been reported *in vivo* [49].

In vivo studies using quinolones such as enrofloxacin and ciprofloxacin have highlighted the emergence of non-growing bacteria that survive treatment in the mesenteric and caecal lymph nodes, often termed persister cells [6, 34-35, 50]. In these studies, fluoroquinolones were used very soon after inoculation, and at high doses (8mg/mouse enrofloxacin oral in [34]; 2.4 mg/mouse ciprofloxacin intraperitoneal in [35]). Fluoroquinolones are known to retain their cidal activity against non-replicating bacteria *in vitro*, hence additional factors such as the high antibiotic concentration or low oxygen tension *in vivo* could be responsible for the emergence of persister bacteria in the gut-associated lymphatic tissues [51-52].

644 Helaine *et al.* [34] used a fluorescence dilution (FD) technique to explore the replication history
645 of individual bacteria during exposure to early, high-dose enrofloxacin in different tissues.
646 They identified persister bacterial populations in the lymph nodes and spleen. Our modelling
647 study indicates that the spleen and MLN are indeed the main sites of interest regarding the
648 emergence of persisters, when mice were treated with ampicillin. However, our model did not
649 predict this persisting subpopulation in ciprofloxacin-treated mice. This discrepancy could
650 either be due to the low levels of persisters in this group, which would not affect the ITS
651 distributions significantly enough to be detected by our model, or due to the differences in the
652 experimental design of the studies, especially the timing and dose of the fluoroquinolone
653 therapy, which is known to affect its pharmacokinetic properties [51]. Our findings suggest
654 that at clinically relevant doses, non-growing "persisters" may not be a universal sequela of
655 antibiotic treatment, but may be antibiotic-specific, as our SP-model was still adequate to
656 capture the dynamics in the ciprofloxacin-treated group. Alternatively, the vast majority of
657 persister bacteria following quinolone exposure may originate from growing instead of non-
658 replicating bacteria [6]. Finally, an important determinant in the apparent lack of consensus in
659 this field is the significant inherent stochasticity in extinction time and dynamics *in vivo* during
660 antibiotic treatment even for large bacterial populations, compounded by host variability [52].
661
662 As noted, the lymph nodes and spleen have been previously identified as organs that harbour
663 non-replicating bacteria recalcitrant to antibiotic activity of beta-lactam antibiotics. Our best-
664 fitting DP model for the ampicillin-treated group further suggests that while this group of
665 persister bacteria originate from bacterial populations originally residing in the spleen and
666 MLN, they have migratory potential. In particular, these non-growing bacteria migrate from
667 the spleen to the liver later during the treatment, and interestingly, once in the liver they convert
668 back to the original phenotype, regaining their replicative capacity, but also their sensitivity to
669 antibiotic killing. While the trigger of the switch is unknown at this stage, one candidate
670 mechanism could be the change in bacterial microenvironment due to inter-tissue migration,
671 particularly the change in occupied host cell type. In a recent *in vivo* study of splenocytes
672 infected with *S.* Typhimurium at the single cell level, Kanvatirth *et al.* [16] showed that
673 different host cell types affect not only how easily *Salmonellae* can replicate or become a target
674 for killing intracellularly, but also how readily they enter a low metabolic, persister state. In
675 contrast to the intimate relationship between the liver and the spleen, recalcitrant bacteria
676 arising in the MLN do not appear to migrate either in the liver or spleen, similar to their growing,
677 antibiotic-sensitive counterparts in that regard. As a result, the MLN stands in isolation,

showing distinct dynamics, while the liver and spleen form a network supporting continuous inter-organ migration.

During the relapse phase, following withdrawal of antibiotic therapy, bacteria resume growth and repopulate the liver, spleen and MLN. In the livers of ampicillin-treated mice where the antibiotic-sensitive and antibiotic-recalcitrant subpopulations co-exit, the former is killed at higher rates despite replicating at lower rates than the latter, collectively leading to its extinction. As a result, all three tissues are repopulated by progeny of the antibiotic-recalcitrant subpopulation.

Nevertheless, inferences made by our model are subject to three levels of limitations, which we describe here. Limitations at the level of the experimental data include the absence of markers of bacterial metabolic activity and uniquely identifiable persister subpopulations. In terms of our modelling approach, we assumed the simplest case of linear rates describing the underlying dynamics of the experimental system; although simplifying, our assumption is justified by dividing the infection timeline into shorter time intervals and making independent inferences for each, and the fact that we only estimated average rates. We developed and applied a single- and a dual-phenotype model but did not increase the model complexity further to include more than two bacterial phenotypes. Our decision was based on the law of parsimony, whereby the simplest possible model structure that adequately captures the observed data is preferred; this reduces the risk of overfitting and model unidentifiability. Additionally, we pooled the ITS distributions from multiple mice per treatment group per time point, effectively assuming homogeneous host immune responses. Finally, at the level of interpreting our results, we have attributed cidal activity to antibiotic effects, ignoring any baseline immune responses. For the purposes of comparing the effects of the two antibiotics, and if the assumption that the average baseline immune response between the two groups is similar, then the differences in the dynamics of two groups are still largely rightly attributable to the action of the antibiotic in question.

In summary, in this paper we present an integrated approach between experimental data and mechanistic mathematical models in a case of immunologically intact, previously untreated mice infected with *S.* Typhimurium, treated with either ampicillin or ciprofloxacin, and finally allowed to relapse. Our study showcases the value of mechanistic mathematical models in maximising biological insight from experimental data, where previous qualitative inference

only provides limited information. The additional benefit of our data-driven modelling approach is making inferences about processes that cannot be or remain challenging to observe experimentally in a living organism. External validation of our inferential insights would require *in vivo* experimental setups that involve groups independently treated with different antibiotics at clinically relevant regimens, and a reliable marker to discern non-growing, antibiotic-recalcitrant bacteria at all time points. Ideally, fine-scale data on drug penetration in different tissues, local drug concentration gradients and host cell uptake would be needed to determine the exact microenvironment to which bacteria are exposed. Serial sampling of the bacterial load from the same host would eliminate any variation attributable to within-host heterogeneity in immune responses.

Data Availability

The observed moments from the experimental data, and example code required to produce parameter estimates for the SP and DP models, are available at:

https://github.com/myrtovlazaki/DP_SP_model

Conflict of interest

OMR is currently an employee of the GSK Vaccines Institute for Global Health (GVGH), part of the GSK group of companies. This does not alter the authors' adherence to all Journal policies on data and material sharing. The authors have no conflicts of interest to declare.

Funding

MV is jointly funded by a Newnham College Major Studentship and a Vergottis Award from the Cambridge Trust. OR is funded by the ALBORADA Trust. OR and DP acknowledge research Grant BB/M020193 from the BBSRC. The funders had no role in study design, data collection and analysis, decision to publish, or preparation of the manuscript.

References

[1] Center for Disease Control. 2019 Antibiotic Resistance Threats in the United States. Atlanta, GA: U.S. Department of Health and Human Services, CDC; 2019. DOI: 10.15620/cdc:82532.

[2] Kohanski, M. A., Dwyer, D. J., & Collins, J. J. 2010. How antibiotics kill bacteria: from targets to networks. Nature reviews. Microbiology, 8(6), 423–435. DOI: 10.1038/nrmicro2333

[3] Wilson, G. S. and A. A. Miles. 1964. Topley and Wilson's Principles of Bacteriology and Immunity. FreeWilson and Miles, 1964.

[4] Bernatová, S., Samek, O., Pilát, Z., Serý, M., Ježek, J., Jákl, P., Siler, M., Krzyžánek, V., Zemánek, P., Holá, V., Dvořáčková, M., & Růžička, F. 2013. Following the mechanisms of bacteriostatic versus bactericidal action using Raman spectroscopy. Molecules (Basel, Switzerland), 18(11), 13188–13199. DOI:10.3390/molecules181113188

[5] McCall IC, Shah N, Govindan A, Baquero F, Levin BR. 2019. Antibiotic killing of diversely generated populations of nonreplicating bacteria. Antimicrob Agents Chemother 63:e02360-18. DOI: 10 .1128/AAC.02360-18.

[6] Claudi, B., Spröte, P., Chirkova, A., Personnic, N., Zankl, J., Schürmann, N., Schmidt, A., & Bumann, D. 2014. Phenotypic Variation of Salmonella in Host Tissues Delays Eradication by Antimicrobial Chemotherapy. Cell, 158(4), 722–733. DOI: 10.1016/j.cell.2014.06.045

[7] Bumann, D., & Cunrath, O. 2017. Heterogeneity of Salmonella-host interactions in infected host tissues. Current Opinion in Microbiology, 39, 57–63. DOI: 10.1016/j.mib.2017.09.008

[8] Dewachter, L., Fauvart, M., & Michiels, J. 2019. Bacterial Heterogeneity and Antibiotic Survival: Understanding and Combatting Persistence and Heteroresistance. Molecular Cell, 76(2), 255–267. DOI: 10.1016/j.molcel.2019.09.028

[9] Haugan, M. S., Charbon, G., Frimodt-Møller, N., & Løbner-Olesen, A. 2018. Chromosome replication as a measure of bacterial growth rate during Escherichia coli infection in the mouse peritonitis model. Scientific Reports, 8(1). DOI: 10.1038/s41598-018-33264-7

[10] Shehata, T. E., & Marr, A. G. 1971. Effect of nutrient concentration on the growth of Escherichia coli. Journal of bacteriology, 107(1), 210–216.

[11] Grant, A. J., Restif, O., McKinley, T. J., Sheppard, M., Maskell, D. J., & Mastroeni, P. 2008. Modelling within-host spatiotemporal dynamics of invasive bacterial disease. PLoS biology, 6(4), e74. DOI: 10.1371/journal.pbio.0060074

[12] Gjini, E., & Brito, P. H. 2016. Integrating Antimicrobial Therapy with Host Immunity to Fight Drug-Resistant Infections: Classical vs. Adaptive Treatment. PLOS Computational Biology, 12(4), e1004857. DOI: 10.1371/journal.pcbi.1004857

[13] Duneau, D., Ferdy, J. B., Revah, J., Kondolf, H., Ortiz, G. A., Lazzaro, B. P., & Buchon, N. 2017. Stochastic variation in the initial phase of bacterial infection predicts the probability of survival in D. melanogaster. eLife, 6, e28298. DOI: 10.7554/eLife.28298

[14] Bottery, M. J., Passaris, I., Dytham, C., Wood, A. J., & van der Woude, M. W. 2019. Spatial Organization of Expanding Bacterial Colonies Is Affected by Contact-Dependent Growth Inhibition. Current Biology, 29(21), 3622–3634.e5. DOI: 10.1016/j.cub.2019.08.074

[15] Kolter, R., Siegele, D. A., & Tormo, A. 1993. The stationary phase of the bacterial life cycle. Annu. Rev. Microbiol. 47, 855–874. DOI: 10.1146/annurev.mi.47.100193.004231

[16] Kanvatirth P., Rossi O., Restif O., Blacklaws B.A., Tonks P., Grant A.J., & Mastroeni P. 2020. The dual role of splenic mononuclear and polymorphonuclear cells in the outcome of ciprofloxacin treatment of Salmonella enterica infections. Manuscript awaiting publication

[17] Kaldalu, N., Hauryliuk, V., & Tenson, T. 2016. Persisters-as elusive as ever. Applied microbiology and biotechnology, 100(15), 6545–6553. DOI: 10.1007/s00253-016-7648-8

[18] Bigger J. W. 1944. Treatment of staphylococcal infections with penicillin by intermittent sterilisation. Lancet 244 497–500. DOI: 10.1016/S0140-6736(00)74210-3

[19] Kim, J.-S., & Wood, T. K. 2016. Persistent Persister Misperceptions. Frontiers in Microbiology, 7. DOI: 10.3389/fmicb.2016.02134

[20] Nielsen EI, Cars O, Friberg LE. 2011. Predicting in vitro antibacterial efficacy across experimental designs with a semimechanistic pharmacokinetic-pharmacodynamic model. Antimicrobial Agents and Chemotherapy 55:1571–1579. DOI: 10.1128/AAC.01286-10

[21] Ferro BE, van Ingen J, Wattenberg M, van Soolingen D, Mouton JW. 2015. Time-kill kinetics of antibiotics active against rapidly growing mycobacteria. Journal of Antimicrobial Chemotherapy 70:811–817. DOI: 10.1093/jac/dku431, PMID: 25344808

[22] Regoes RR, Wiuff C, Zappala RM, Garner KN, Baquero F, Levin BR. 2004. Pharmacodynamic functions: A multiparameter approach to the design of antibiotic treatment regimens. Antimicrobial Agents and Chemotherapy 48:3670–3676. DOI: 10.1128/AAC.48.10.3670-3676.2004

[23] Haugan, M. S., Løbner-Olesen, A., & Frimodt-Møller, N. 2018. Comparative Activity of Ceftriaxone, Ciprofloxacin, and Gentamicin as a Function of Bacterial Growth Rate Probed by Escherichia coli Chromosome Replication in the Mouse Peritonitis Model. Antimicrobial Agents and Chemotherapy, 63(2), e02133-18. DOI: 10.1128/aac.02133-18

[24] Fantin, B., Ebert, S., Leggett, J., Vogelman, B., & Craig, W. A. 1991. Factors affecting duration of in-vivo postantibiotic effect for aminoglycosides against Gram-negative bacilli. Journal of Antimicrobial Chemotherapy, 27(6), 829–836. DOI: 10.1093/jac/27.6.829

[25] Zeiler HJ, Voigt WH. 1987. Efficacy of ciprofloxacin in stationary-phase bacteria in vivo. The American Journal of Medicine. Apr;82(4A):87-90.

[26] Ghooi, R. B., & Thatte, S. M. 1995. Inhibition of cell wall synthesis — is this the mechanism of action of penicillins? Medical Hypotheses, 44(2), 127–131. DOI: 10.1016/0306-9877(95)90085-3

[27] Lee, A. J., Wang, S., Meredith, H. R., Zhuang, B., Dai, Z., & You, L. (2018). Robust, linear correlations between growth rates and β-lactam–mediated lysis rates. Proceedings of the National Academy of Sciences, 115(16), 4069–4074. DOI : 10.1073/pnas.1719504115

[28] Tuomanen, E., Cozens, R., Tosch, W., Zak, O., & Tomasz, A. 1986. The Rate of Killing of Escherichia coli by -Lactam Antibiotics Is Strictly Proportional to the Rate of Bacterial Growth. Microbiology, 132(5), 1297–1304. DOI : 10.1099/00221287-132-5-1297

[29] Yao, Z., Kahne, D., & Kishony, R. 2012. Distinct Single-Cell Morphological Dynamics under Beta-Lactam Antibiotics. Molecular Cell, 48(5), 705–712. DOI : 10.1016/j.molcel.2012.09.016

[30] Ocampo, P. S., Lázár, V., Papp, B., Arnoldini, M., Abel zur Wiesch, P., Busa-Fekete, R., … Bonhoeffer, S. 2014. Antagonism between Bacteriostatic and Bactericidal Antibiotics Is Prevalent. Antimicrobial Agents and Chemotherapy, 58(8), 4573–4582. DOI: 10.1128/aac.02463-14

[31] Cui, P., Niu, H., Shi, W., Zhang, S., Zhang, W., & Zhang, Y. 2018. Identification of Genes Involved in Bacteriostatic Antibiotic-Induced Persister Formation. Frontiers in Microbiology, 9. DOI : 10.3389/fmicb.2018.00413

[32] Drlica, K., Malik, M., Kerns, R. J., & Zhao, X. 2007. Quinolone-Mediated Bacterial Death. Antimicrobial Agents and Chemotherapy, 52(2), 385–392. DOI: 10.1128/aac.01617-06

[33] Sanders, C. C. 1988. Ciprofloxacin: In Vitro Activity, Mechanism of Action, and Resistance. Clinical Infectious Diseases, 10(3), 516–527. DOI: 10.1093/clinids/10.3.516

[34] Helaine, S., Cheverton, A. M., Watson, K. G., Faure, L. M., Matthews, S. A., & Holden, D. W. 2014. Internalization of Salmonella by Macrophages Induces Formation of Nonreplicating Persisters. Science, 343(6167), 204–208. DOI: 10.1126/science.1244705

[35] Kaiser, P., Regoes, R. R., Dolowschiak, T., Wotzka, S. Y., Lengefeld, J., Slack, E., Grant, A. J., Ackermann, M., & Hardt, W.-D. 2014. Cecum Lymph Node Dendritic Cells Harbor Slow-Growing Bacteria Phenotypically Tolerant to Antibiotic Treatment. PLoS Biology, 12(2), e1001793. DOI: 10.1371/journal.pbio.1001793

[36] Diard, M., Sellin, M. E., Dolowschiak, T., Arnoldini, M., Ackermann, M., & Hardt, W.-D. 2014. Antibiotic Treatment Selects for Cooperative Virulence of Salmonella Typhimurium. Current Biology, 24(17), 2000–2005. DOI: 10.1016/j.cub.2014.07.028

[37] Bakkeren, E., Huisman, J. S., Fattinger, S. A., Hausmann, A., Furter, M., Egli, A., … Hardt, W.-D. 2019. Salmonella persisters promote the spread of antibiotic resistance plasmids in the gut. Nature, 573(7773), 276–280. DOI: 10.1038/s41586-019-1521-8

[38] Rossi, O., Dybowski, R., Maskell, D. J., Grant, A. J., Restif, O., & Mastroeni, P. 2017. Within-host spatiotemporal dynamics of systemic Salmonella infection during and after antimicrobial treatment. Journal of Antimicrobial Chemotherapy, 72(12), 3390–3397. DOI: 10.1093/jac/dkx294

[39] Gollan, B., Grabe, G., Michaux, C., & Helaine, S. 2019. Bacterial Persisters and Infection: Past, Present, and Progressing. Annual Review of Microbiology, 73(1), 359–385. DOI: 10.1146/annurev-micro-020518-115650

[40] Balaban, N. Q. 2004. Bacterial Persistence as a Phenotypic Switch. Science, 305(5690), 1622–1625. DOI : 10.1126/science.1099390

[41] Carpenter JW. Exotic Animal Formulary. London: Saunders, 2012.

[42] Hawk CT, Leary SL, Morris TH et al. Formulary for Laboratory Animals. Oxford: Blackwell, 2005.

[43] Markov A.A.. 1906. Extension of the law of large numbers to dependent quantities (in Russian). Izvestiia Fiz.-Matem. Obsch. Kazan Univ., (2nd Ser.), 15(1906)

[44] Price, D. J., Breuzé, A., Dybowski, R., Mastroeni, P., & Restif, O. 2017. An efficient moments-based inference method for within-host bacterial infection dynamics. PLOS Computational Biology, 13(11), e1005841. DOI: 10.1371/journal.pcbi.1005841

[45] Price, D. J. & Restif, O. 2017. SPEEDI.R - Simulation Package for Efficient Experimental Design and Inference in R. https://github.com/orestif/SPEEDI.R

[46] Nelder, J. A., & Mead, R. (1965). A Simplex Method for Function Minimization. The Computer Journal, 7(4), 308–313. DOI: 10.1093/comjnl/7.4.308

[47] Landman, D. 1997. Management of infections due to resistant enterococci: a review of therapeutic options. Journal of Antimicrobial Chemotherapy, 40(2), 161–170. https://doi.org/10.1093/jac/40.2.161

[48] Diard, M., Sellin, M. E., Dolowschiak, T., Arnoldini, M., Ackermann, M., & Hardt, W.-D. 2014. Antibiotic Treatment Selects for Cooperative Virulence of Salmonella Typhimurium. Current Biology, 24(17), 2000–2005. DOI: 10.1016/j.cub.2014.07.028

[49] Lewis, K. 2010. Persister Cells. Annual Review of Microbiology, 64(1), 357–372. DOI: 10.1146/annurev.micro.112408.134306

[50] Griffin, A. J., Li, L.-X., Voedisch, S., Pabst, O., & McSorley, S. J. 2011. Dissemination of Persistent Intestinal Bacteria via the Mesenteric Lymph Nodes Causes Typhoid Relapse. Infection and Immunity, 79(4), 1479–1488. DOI: 10.1128/iai.01033-10

[51] Lewin, C. S., Morrissey, I., & Smith, J. T. 1991. The mode of action of quinolones: The paradox in activity of low and high concentrations and activity in the anaerobic environment. European Journal of Clinical Microbiology & Infectious Diseases, 10(4), 240–248. DOI: 10.1007/bf01966996 [45] Bumann and Cunrath, 2017

[52] Coates, J., Park, B. R., Le, D., Şimşek, E., Chaudhry, W., & Kim, M. 2018. Antibiotic-induced population fluctuations and stochastic clearance of bacteria. eLife, 7, e32976. DOI: 10.7554/eLife.32976